25th ABCM International Congress of Mechanical Engineering
October 20-25, 2019, Uberlândia, MG, Brazil

COB-2019-0678
ANALYSIS OF THERMOHYDRODYNAMIC MODELS FOR THE BEARINGS OF A FRANCIS HYDROPOWER UNIT

Jefferson Silva Barbosa
Leonardo Campanine Sicchieri
Aldemir Aparecido Cavalini Jr
Valder Steffen Jr
LMEst, Structural Mechanics Laboratory, Federal University of Uberlândia, School of Mechanical Engineering, Av. João Naves de Ávila, 2121, 38408-196, Uberlândia, Brazil
jsbarbosa@ufu.br, leo_sicchieri@ufu.br, aacjunior@ufu.br, vsteffen@ufu.br

Abstract. *This work is dedicated to the computational modeling of the hydrodynamic bearings present in a Francis hydropower unit. A thermohydrodynamic approach is used to represent the dynamic behavior of these bearings, in which the thermal effects due to the viscous friction of the oil film are computed through the simultaneous solution of the Reynolds and energy equations. Using simplifying hypotheses, three hydrodynamic bearings of the hydropower unit are analyzed, namely tilting-pad thrust bearing, tilting-pad journal bearing, and cylindrical journal bearing. The representativeness of the numerical results obtained in the present work, they were verified using the corresponding data provided by the manufacturer. Good correlation between both information could be observed. It is worth mentioning that the present work was developed under the R&D project Robust Modeling for the Diagnosis of Defects in Generating Units (02476-3108/2016) conducted by ANEEL (Brazilian Electric Energy Agency). This project is carried out at the Federal University of Uberlândia, Brazil, with the financial support of the companies CERAN, BAESA, ENERCAN, Foz do Chapecó, and CPFL Energia.*

Keywords: *hydrodynamic bearings, thermohydrodynamic models, Francis hydropower unit.*

1. INTRODUCTION

Bearings are mechanical elements responsible for supporting rotating shafts, which can be axial or radial (thrust or journal bearings, respectively), depending on the direction of the applied load (Dourado et al., 2019). Bearings can be further classified as a roller (or ball), hydrodynamic, and magnetic bearings. Hydrodynamic bearings can present fixed or variable geometries, such as the tilting-pad bearings. These bearings are widely applied in the industry and show satisfactory stability, allowing to operate in higher rotating speeds (Barbosa, 2018). Hydrodynamic bearings are commonly used in hydropower units due to their load capabilities (Vance, Zeidan, and Murphy, 2010).

The mathematical simulation of hydropower units is an indispensable resource for engineers, allowing a comprehensive understanding of the dynamic behavior of the system and prediction of undesired operating conditions (Dourado et al., 2019). In this context, the development of models for representing hydrodynamic bearings becomes mandatory.

The theoretical studies of Osborn Reynolds (Reynolds, 1886) resulted in a partial differential equation obtained from simplifications applied to the Navier-Stokes equation. The pressure field in the oil film can be determined by solving the Reynolds equation. In the approach proposed by Reynolds (1886), the oil film temperature is considered constant. However, due to the motion between the bearing parts, part of the kinetic energy is converted into thermal energy. The oil temperature increases and, consequently, the oil viscosity decreases. Aiming to obtain accurate hydrodynamic bearing models, Dowson (1962) solved the Reynolds equation considering changes in the oil film temperature. In this thermohydrodynamic model (THD), the thermal effects were considered by associating the energy equation with the modified Reynolds equation.

The Francis hydropower unit considered in the present work is composed by a vertical shaft, a generator unit, a Francis turbine, and three bearings, namely a combined tilting-pad thrust/journal bearing located at the top of the generator, a tilting-pad journal bearing located at the bottom of the generator, and a cylindrical journal bearing located close to the Francis turbine. Is this work, THD models are applied for determining the pressure and temperature fields in the three hydrodynamic bearings of the considered hydropower unit. The maximum pressure, maximum temperature, and minimum oil film thickness are also determined.

2. THD BEARING MODEL

In this section, the THD models used to represent the tilting-pad thrust bearing (TPTB), the tilting-pad radial bearing (TPJB), and the cylindrical journal bearing (CJB) of the Francis hydropower unit are presented. The equilibrium condition for the considered models was obtained by equating the external load applied to the bearings with the hydrodynamic forces, which were determined by integrating the pressure distribution over the projected area of the bearings. The equilibrium of momentum was also achieved for the TPTB and TPJB. The pressure and the temperature fields generated in the oil film were obtained. Details on the THD models for the considered hydrodynamic bearings can be found in Barbosa (2018).

2.1 Tilting pad thrust bearing

Figure 1 illustrates the physical model of the TPTB. In this case, the pad inner and outer radii are given by r_1 and r_2, respectively, θ_{pivot} and r_{pivot} are the angular and radial positions of the pivot, respectively, θ_0 stands for the pad angular length, α_p and α_r are the pad rotational angles at the pivot along the r and s directions, respectively, and h_h is the oil film thickness.

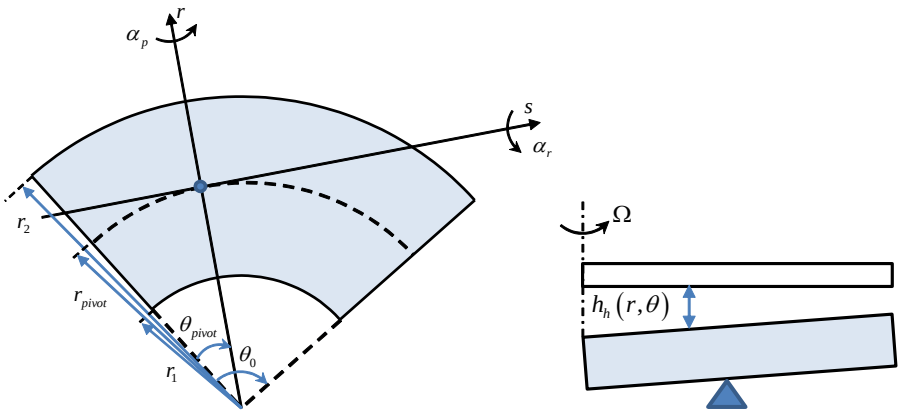

Figure 1. Physical model of the TPTB.

The hydrodynamic forces are determined by calculating the equilibrium position of the bearing. For this aim, the angles α_p and α_r and the oil film thickness at the pivot h_0 should be obtained, as shown in Eq. (1) and Eq. (2).

$$\mathbf{X} = \begin{bmatrix} h_0 & \alpha_r & \alpha_p \end{bmatrix} \tag{1}$$

$$\begin{aligned} f_1 &= \mathbf{F}_Y + \mathbf{F}_w \rightarrow 0 \\ f_2 &= M_r = \int_{r_1}^{r_2}\int_{\theta_1}^{\theta_2} p_h \cdot r^2 \cdot \sin\left(\theta - \theta_{pivot}\right) \cdot d\theta \cdot dr \rightarrow 0 \\ f_3 &= M_s = \int_{r_1}^{r_2}\int_{\theta_1}^{\theta_2} p_h \cdot r\left(r \cdot \cos\left(\theta - \theta_{pivot}\right) - r_{pivot}\right) \cdot d\theta \cdot dr \rightarrow 0 \end{aligned} \tag{2}$$

Equation (1) represents the vector of design variables that are to be determined. $\mathbf{F}_Y$ and $\mathbf{F}_w$ are the hydrodynamic force and external loading, respectively, f_1 stands for the equilibrium of forces, f_2 and f_3 refer to the equilibrium of momentum along the directions r and s, respectively. Figure 2 shows the flowchart regarding the iterative process associated with the THD-TPTB model.

2.2 Tilting pad journal bearing

Figure 3 presents the schematic representation of a TPJB. In this case, Ω is the rotation speed of the shaft, R is the shaft radius, R_S is pad radius, O_P, O_E, and O_S are the pivot center of rotation, shaft center, and pad center, respectively, h_0 is the bearing radial clearance, and α is the pad angle relative to the pivot.

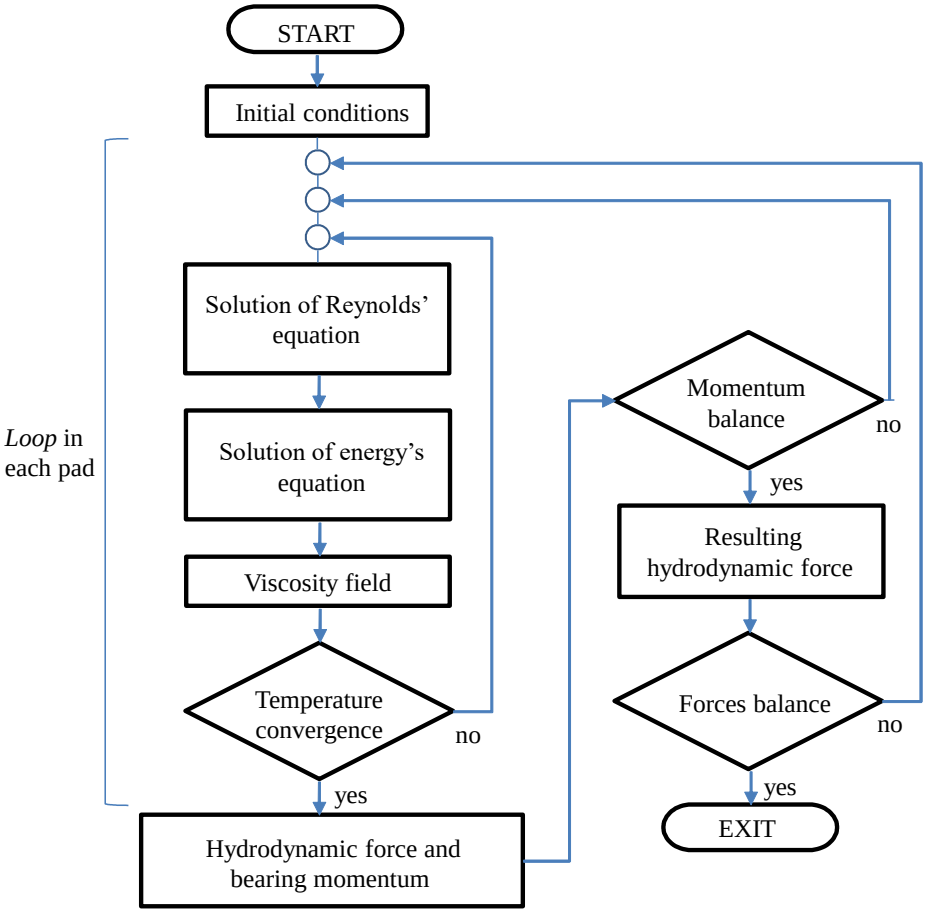

Figure 2. Procedure for determine the hydrodynamic forces in TPTB (Barbosa, 2018, adapted).

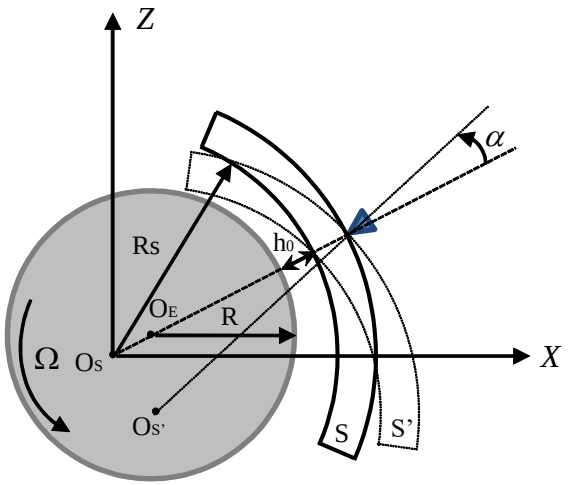

Figure 3. Physical model of the TPJB.

The hydrodynamic supporting forces in TPJB are determined at the equilibrium positions of the shaft and the pads (equilibrium of momentum). The position of the shaft center $O_E\,(X_r, Z_r)$ and the angle α of each pad can be determined, as given by Eq. (3) and Eq. (4).

$$\mathbf{X} = \left[X_r \quad Z_r \quad \alpha_1 \quad \alpha_2 \quad \ldots \quad \alpha_N \right] \tag{3}$$

$$f_1 = \mathbf{F}_R + \mathbf{F}_w \rightarrow 0$$
$$f_2 = M_{R_1} = F_{xm_1} \cdot \left(R_S + h_S\right) \rightarrow 0 \tag{4}$$
$$f_3 = M_{R_2} = F_{xm_2} \cdot \left(R_S + h_S\right) \rightarrow 0 \quad \ldots \quad f_{N+1} = M_{R_N} = F_{xm_N} \cdot \left(R_S + h_S\right) \rightarrow 0$$

Equation (3) represents the vector of design variables that should be obtained. In Eq. (4), $\mathbf{F}_R$ and $\mathbf{F}_w$ are the hydrodynamic force and external load, respectively, f_1 stands for the equilibrium of forces, and f_2, f_3, … f_{N+1} represents the equilibrium of momentum. Figure 4 shows the flowchart concerning the procedure for determining the hydrodynamic forces according to the THD-TPJB model.

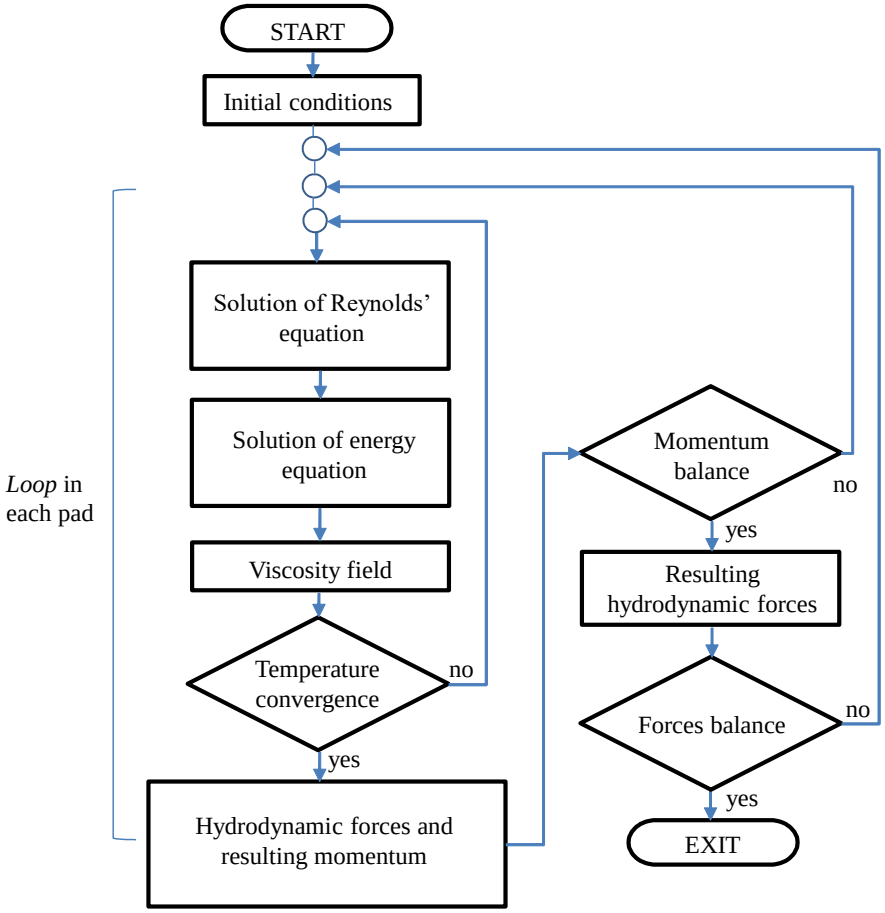

Figure 4. Procedure for determining the hydrodynamic forces in TPJB. (Barbosa, 2018, adapted).

2.3 Cylindrical journal bearing

Figure 5 presents the main geometric parameters of the CJB. In this case, R is the shaft radius, L_h is the bearing length, C is the radial clearance, e is the eccentricity (radial displacement from the center of the shaft O_E to the center of the bearing), α_h is the angle that defines the angular position of the shaft center, and Ω is the rotation speed of the shaft.

The hydrodynamic supporting forces in CJB are determined at the equilibrium position of the shaft. The position of the shaft center O_E (X_r, Z_r) should be determined, as shown in Eq. (5) and Eq. (6).

$$\mathbf{X} = \begin{bmatrix} E & \alpha_h \end{bmatrix} \tag{5}$$

$$f_1 = \mathbf{F}_w + \mathbf{F}_h \rightarrow 0 \tag{6}$$

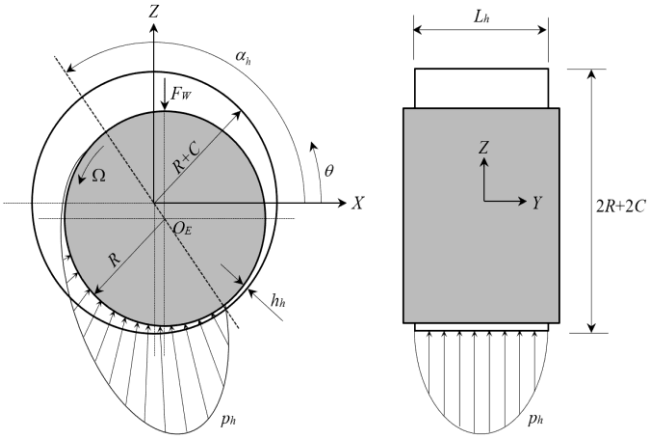

Figure 5. Physical model of the CJB (Cavalini Jr et al., 2017, adapted).

Equation (5) represents the vector of design variables that should be determined. In Eq. (6), $\mathbf{F}_h$ and $\mathbf{F}_w$ are the hydrodynamic force and external load, respectively, and f_1 refers to the equilibrium of forces. Figure 6 shows the flowchart concerning the procedure for determining the hydrodynamic forces according to the THD-CJB model.

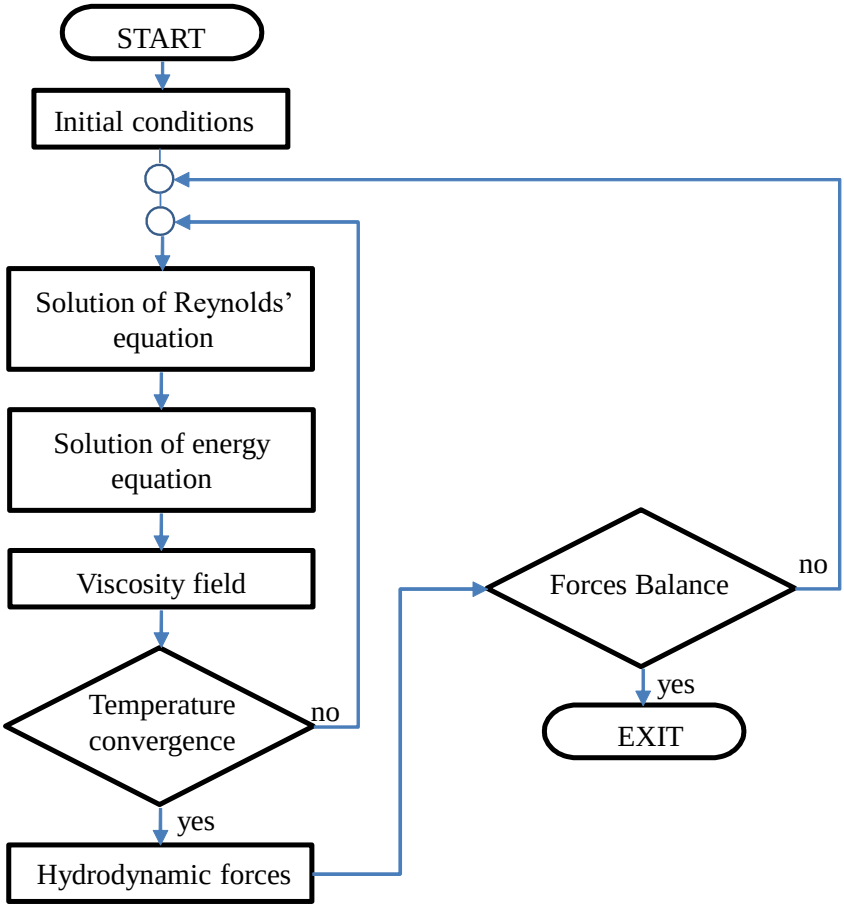

Figure 6. Procedure for determining the hydrodynamic forces in CJB (Barbosa, 2018, adapted).

3. NUMERICAL RESULTS

This section is dedicated to the numerical results obtained by using the THD models of the considered hydrodynamic bearings. There are particularities regarding the geometry and lubrication form of each bearing, which are detailed next. It is important to note that the operating conditions considered for the bearings were provided by the manufacturer of the Francis hydropower unit.

Figure 7 shows the location of the bearings in the considered hydropower unit. This machine presents 44.58 MW nominal power, operates at 300 rpm, 24 poles generator, 60 Hz frequency, 13,800 V voltage, and 2,027.5 A current.

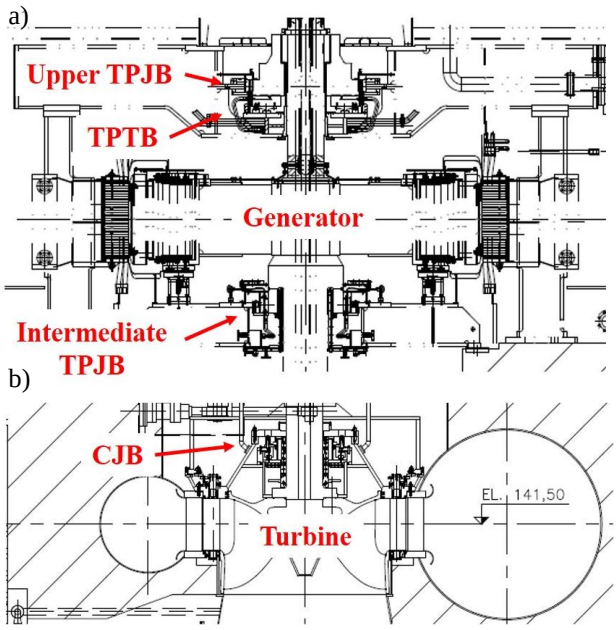

Figure 7. Francis hydropower unit: a) Upper part of the machine; b) Bottom part of the machine (Barbosa, 2018, adapted).

3.1 Tilting-pad thrust bearing

Table 1 presents the geometric properties and operating parameters of the TPTB. Table 2 shows the results obtained by using the implemented THD-TPTB model. The results provided by the manufacturer are also presented for comparison purposes. Note that similar results were obtained, which demonstrates the representativeness of the implemented THD-TPTB model. Figure 8 shows the associated pressure and temperature fields.

Table 1. Geometric properties and operating parameters of the TPTB.

Parameters	Values
Inner radius	310 mm
Outer radius	660 mm
Pivot radius	485 mm
Pad angle	45°
Number of pads	6
Arc pivot/arc pad	0.6
Rotation speed	300 rpm
Oil type	ISO VG 68
Load bearing	2300 kN

Table 2. Results obtained with the THD-TPTB model and provided by the manufacturer.

Properties	Manufacturer	Present work	Difference (%)
P_{max} (MPa)	6.90	6.93	0.43
T_{max} (GPa)	69.25	64.51	6.84
h_{min} (μm)	58.79	50.65	13.85

It is important to note in Fig. 8a, Fig. 8b, and Fig. 8c that the region of the pad in which the hydrodynamic pressure has a maximum magnitude is located on the right side of the pad. This effect is due to the rotation direction of the shaft. Additionally, the region of maximum temperature (see Fig. 8d and Fig. 8e) is observed in the upper right part of the pad due to advection heat transfer mechanism (velocity components along with the directions θ and r).

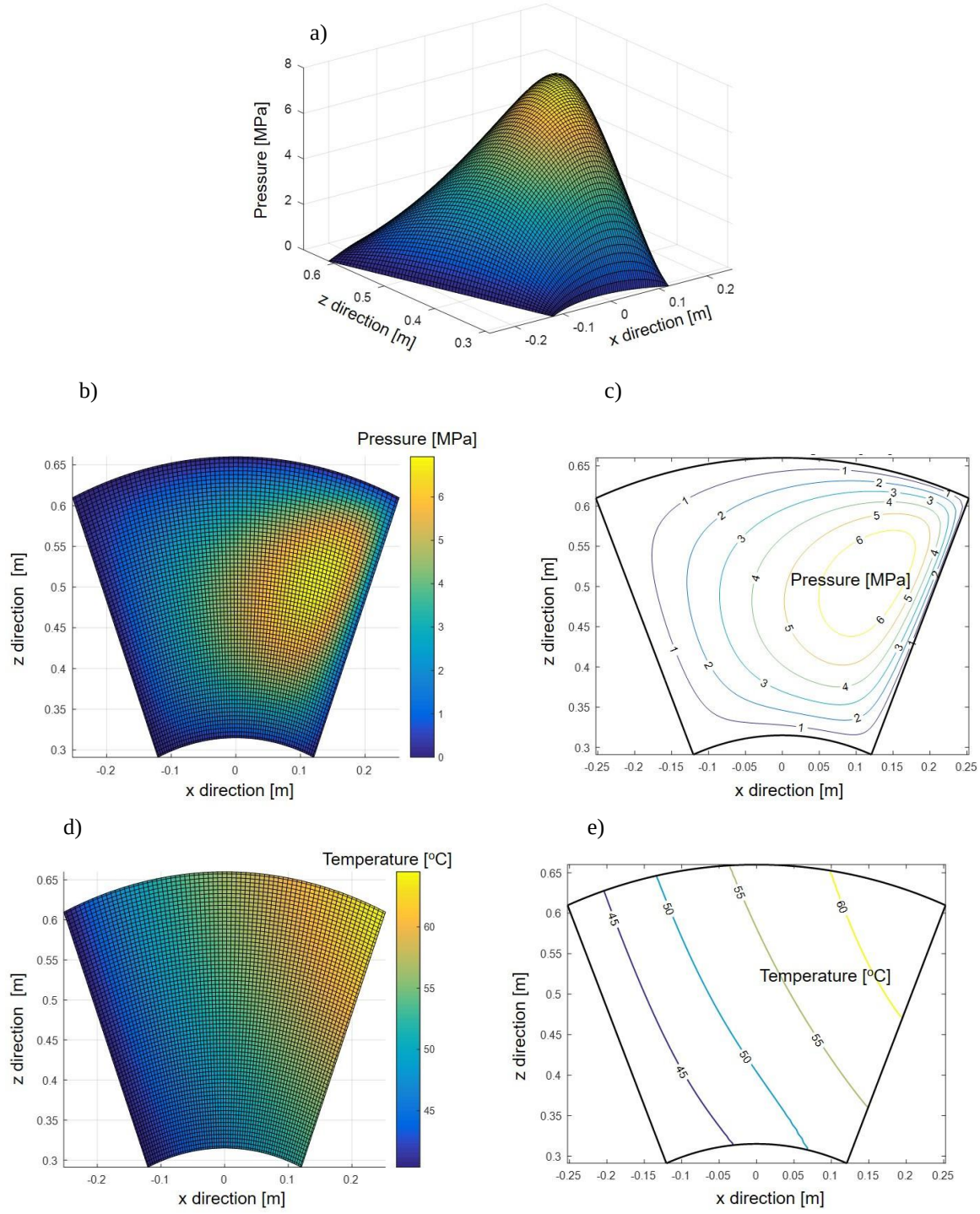

Figure 8. Pressure and temperature fields of the TPTB. a) 3D Pressure field; b) Upper view of pressure field; c) Lines of constant pressure; d) 2D Temperature field; e) Lines of constant temperature (Barbosa, 2018).

3.2 Tilting-pad journal bearing

Figure 9 presents one of the pads of the considered TPJB. In this bearing, zone 1 corresponds to the oil recess, whereby part of the lubricant flows to the oil reservoir. In this region, it is assumed that the manometric pressure is null. Zone 3 refers to the active region of the bearing, in which the pressure field is developed. Zone 4 also corresponds to the oil outlet. The pivot point of the pad is represented by 2. The parameters related to the TPJB are shown in Tab. 3.

Table 4 shows the results obtained by using the implemented THD-TPJB model. The data provided by the manufacturer are also presented for comparison purposes.

Table 3. Geometric properties and operating parameters of the TPJB.

Parameters	Values
Inner diameter	934 mm
Shaft diameter	930 mm
Radial clearance	250 µm
Length of bearing	197 mm
Pad thickness	67 mm
Pad angle	60°
Number of pads	6
Arc pivot/arc pad	0.6
Angular position of the pivots in the bearing	0°/60°/120°/180°/240°/300°
Rotation speed	300 rpm
Oil type	ISO VG 68
Load bearing	90.6 kN

Table 4. Results obtained with the THD-TPJB model and provided by the manufacturer.

Properties	Manufacturer	Present work	Difference (%)
P_{max} (MPa)	4.761	4.767	0.13
T_{max} (GPa)	52.84	56.40	6.74
h_{min} (µm)	72.70	75.67	4.09

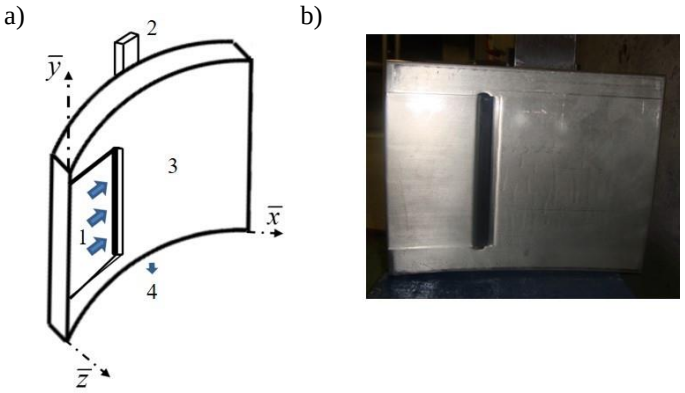

Figure 9. Representation of the TPJB. a) Regions of the bearing; b) Inner surface of the TPJB. (Barbosa, 2018).

Note that similar results were obtained, which demonstrates the representativeness of the implemented THD-TPJB model. Figure 10 presents the associated pressure and temperature fields.

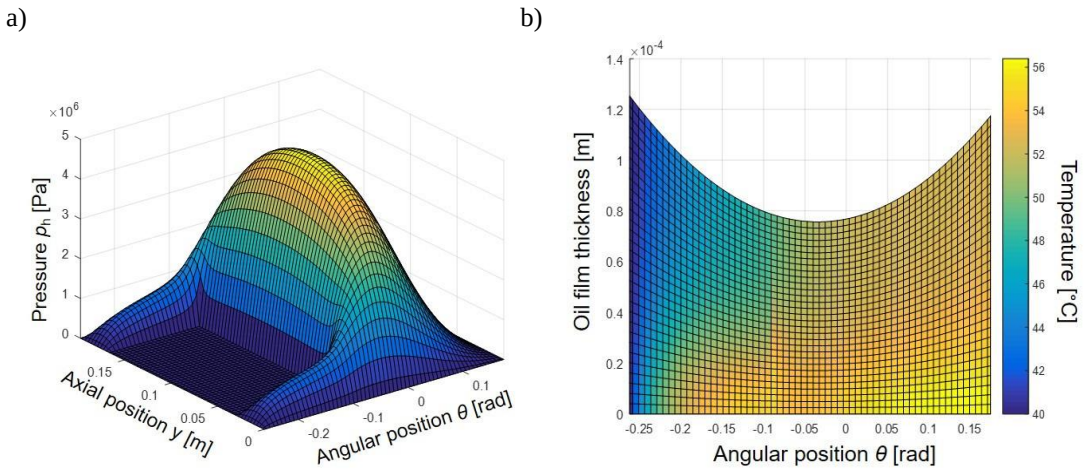

Figure 10. Pressure and temperature fields for the TPJB. a) Pressure field; b) Temperature field (Barbosa, 2018).

3.3 Cylindrical journal bearing

Figure 11 shows one part of the considered CJB (two-part bearing). In this bearing, zone 1 corresponds to the mixing region between the heated and cold oil, which is injected into the bearing through the hole outlined in 3. Zone 2 corresponds to a recess, where the oil coming from the mixing region flows to the active zone of the bearing (zone 4).

a) b)

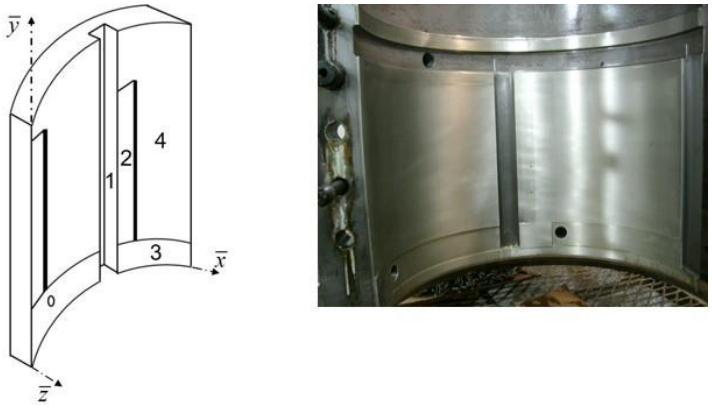

Figure 11. Representation of CJB. a) Regions of the bearing; b) Internal surface of the CJB (Barbosa, 2018).

Note that there are four cold oil injection holes, four mixing regions, and four recesses. The pressure on zones 1, 2, and 3 are considered null since the thickness of the oil film in these regions is much larger than in the active ones. Therefore, the pressure field in these regions is significantly lower as compared to the active zones of the bearing. The parameters of the CJB are shown in Tab. 5. Note that three different operating conditions were provided by the manufacturer.

Table 5. Geometric properties and operating parameters of the CJB.

Parameters	Values
Inner diameter	550.4 mm
Shaft diameter	550 mm
Radial clearance	200 μm
Length of the bearing (active zone)	330 mm
Rotation speed	300 rpm
Oil type	ISO VG 68
Operating condition #1	81.5 kN at 300 rpm
Operating condition #2	188 kN at 583 rpm
Operating condition #3	219 kN at 300 rpm

The maximum pressure, maximum temperature, and minimum oil film thickness for the three different operating conditions presented in Tab. 5 are shown in Tab. 6. Note that the maximum pressure increases according to the external load, as well as the shaft eccentricity E and its angular position α_h. As expected, the oil film thickness decreases according to the external load. However, the maximum temperature was achieved for operating condition #2. This result is associated with the considered rotation speed for the shaft.

Table 6. Results obtained with the THD-CJB model.

Operating condition	α_h [°]	E	P_{max} [MPa]	T_{max} [ºC]	h_{min} [μm]
81.5 kN at 300 rpm	34.48	0.392	1.425	68.80	121.56
188 kN at 583 rpm	36.97	0.437	3.425	108.85	112.61
219 kN at 300 rpm	40.81	0.513	4.314	105.03	97.47

Figure 12 presents the associated pressure and temperature fields obtained for condition #1. In this case, the manufacturer omitted the corresponding data. Figure 12a shows the regions where the pressure is null due to the recesses present in zones 1, 2, and 3 of the CJB (see Fig. 11a). In Fig. 12b, it is possible to observe regions in which the oil temperature is low. These regions correspond to the zones where the mixture between the heated and cold oil occurs.

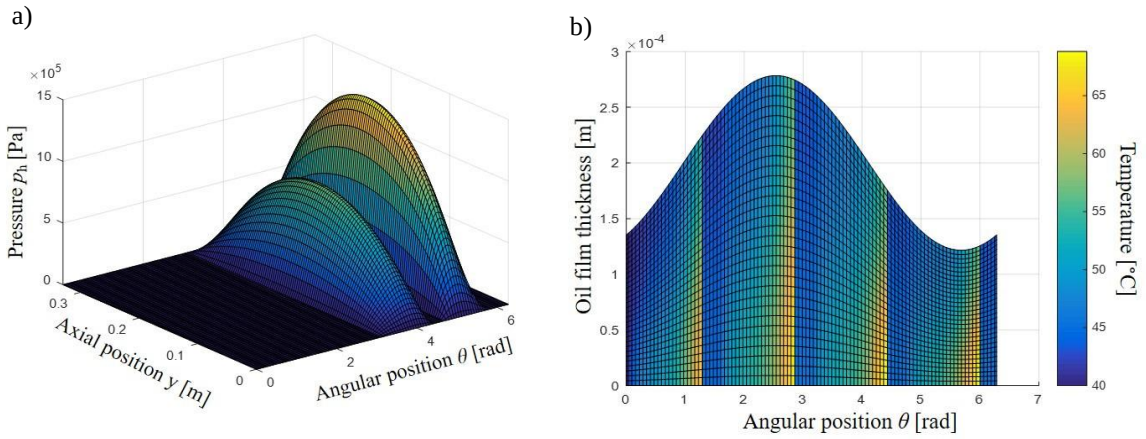

Figure 12. Pressure and temperature field in the CJB. a) Pressure field; b) Temperature field (Barbosa, 2018).

4. FINAL REMARKS

In this work, the hydrodynamic bearings of a Francis hydropower unit were analyzed according to dedicated THD models. In this approach, the pressure and temperature fields, as well as the maximum pressure, maximum temperature, and minimum oil film thickness were determined. The results obtained for the tilting-pad thrust bearing (TPTB) and tilting-pad journal bearing (TPJB) were similar to the data provided by the manufacturer. The results associated with the cylindrical journal bearing (CJB) demonstrated to be physically consistent. Further research work will be dedicated to including these models in the finite element model of the rotating machine. The development of surrogate models for these bearings based on the THD approach is also scheduled.

5. ACKNOWLEDGMENTS

The authors are thankful for the financial support provided to the present research effort by CNPq (574001/2008-5, 304546/2018-8, and 431337/2018-7), FAPEMIG (TEC-APQ-3076-09, TEC-APQ-02284-15, TEC-APQ-00464-16, and PPM-00187-18), and CAPES through the INCT-EIE. The authors are also thankful to the companies CERAN, BAESA, ENERCAN, Foz do Chapecó, and CPFL Energia for the financial support through the R&D project Robust Modeling for the Diagnosis of Defects in Generating Units (02476-3108/2016).

6. REFERENCES

Barbosa, J.S., 2018, “Análise de Modelos Termohidrodinâmicos para Mancais de Unidades Geradoras Francis”, Universidade Federal de Uberlândia, Uberlândia, Brasil, 92 p.

Cavalini Jr., A.A., Silva, A.D.G., Lara-Molina, F.A., Steffen Jr., 2017, “Dynamic Analisys of a Flexible Rotor Supported by Hydrodynamic Bearings with Uncertain Parameters” Meccanica, Vol. 52, pp. 2931-2943.

Dowson, D., 1962, “A Generalized Reynolds Equation for Fluid Film Lubrication” International Journal of Mechanical Sciences, Vol. 4, pp. 159-170.

Dourado, A.P., Barbosa, J.S., Sicchieri, L., Cavalini Jr., A.A., Steffen Jr., V, 2019, “Kriging Surrogate Model Dedicated to a Tilting-Pad Journal Bearing” Proceedings of the 10th International Conference on Rotor Dynamics - IFToMM, Vol.1, Rio de Janeiro, Brazil, pp. 347-358.

Reynolds, O., 1886, “On the Theory of Lubrication and its Application to Mr. Beauchamp Tower’s Experiments, Including an Experimental Determination of the Viscosity of Olive Oil” Philosophical Transactions of Royal Society of London, Vol. 177, pp. 157-234.

Vance, J., Zeidan, F., Murphy, B., 2010, “Machinery Vibration and Rotordynamics”, Wiley, New Jersey.

7. RESPONSIBILITY NOTICE

The authors are the only responsible for the printed material included in this paper.